

Gigantic Ferromagnetic Magneto-Optical Effect in a SiC Light-emitting Diode Fabricated by Dressed-Photon–Phonon- Assisted Annealing

M. Ohtsu¹ and T. Kawazoe²

¹Research Origin for Dressed Photon,
c/o Nichia Corp., 3-13-19 Moriya-cho, Kanagawa-ku, Yokohama, Kanagawa 221-0022 Japan

²Tokyo Denki University,
5 Senju-Asahi-cho, Adachi-ku, Tokyo 120-8551, Japan

Abstract

This paper investigates the gigantic magneto-optical effect in a SiC light-emitting diode fabricated by dressed-photon–phonon (DPP)-assisted annealing. Very large values of the Verdet constant and the Faraday rotation angle were obtained, namely, 660 deg/A and 2480 deg/cm, respectively, at a wavelength of 405 nm. The remanent magnetization was 0.36 mT. The magnetization curve, acquired at 27 °C, exhibited a clear hysteresis characteristic. This behavior of the SiC crystal, equivalent to that of a ferromagnet, was attributed to Al atom pairs autonomously formed as a result of the DPP-assisted annealing.

1 Introduction

Although crystalline silicon (Si) has been popularly used for electronic devices, there is a long-held belief that Si is not suitable for use in light-emitting devices because it is an indirect-transition-type semiconductor, and thus, its emission efficiency is very low. However, dressed-photon–phonon (DPP)-assisted annealing [1] has drastically increased the emission efficiency, resulting in the realization of novel light sources, including light-emitting diodes (LEDs) and lasers [2]. A novel photo-detector with optical gain [3] has also been realized by using crystalline Si. These devices can be advantageously applied to future photonic technology because crystalline Si is a nontoxic, abundant material, and furthermore, these devices can be integrated with electronic devices. Crystalline SiC, another indirect-transition-type semiconductor, has also been used to fabricate LEDs having light emission in the short-wavelength region

with the DPP-assisted annealing [4,5]. In addition to these optical functional devices, an optical polarization rotator using crystalline SiC has been invented [6,7], which can be used as an optical signal modulator. The advent of such novel devices means that conventionally used direct-transition-type composite semiconductors can be replaced by indirect-transition-type semiconductors in the fabrication of the basic devices needed for future optical signal processing and transmission systems.

The present paper investigates the fabrication and operation of an optical polarization rotator using crystalline SiC. The unique phenomenon involved here is that the crystalline SiC exhibits a gigantic magneto-optical effect and also a ferromagnetic characteristic.

2 Device structure

This section briefly describes the SiC device structure for the optical polarization rotator. A detailed description has been given in refs. [4,5]. An n-type 4H-SiC crystal with a resistivity of 25m Ω cm and (0001) surface orientation was used. A 500 nm-thick n-type buffer layer was deposited on this crystal, after which a 10 μ m-thick n-type epitaxial layer (n-type dopant (N atoms) density 1×10^{16} cm⁻³) was deposited. The surface of the 4H-SiC crystal was then implanted with an p-type dopant (Al atoms) by ion implantation. To activate the Al ions for forming a p-n homojunction, thermal annealing was performed for 5 min. at 1800 °C. After this, a second thermal annealing was performed under the same conditions as above.

Although the structure was almost the same as that of the SiC-LED described in refs. [4,5], it was inverted, resulting in the SiC substrate being the top layer. Furthermore, an H-shaped electrode formed of a Cr/Pt/Au (100 nm/150 nm/200 nm thick) stripe film was deposited on the top surface, as shown in Fig. 1(b). A homogeneous electrode formed of Cr/Ni/Au (100 nm/150 nm/200 nm thick) was deposited on the bottom surface. After this, the 4H-SiC crystal was diced to form a device with an area of 500 μ m \times 500 μ m. Figures 1(a) and (b) show the cross-sectional structure of a fabricated device and a photograph of the device taken from above, respectively.

A forward bias voltage of 12 V (current density 45 A/cm²) was applied to the device to bring about annealing due to Joule-heat, which caused the Al atoms to diffuse. During this process, the device was irradiated from the top surface with laser light (optical power 20 mW) having a wavelength of 405 nm. This induced the DPP-assisted

annealing process, which modified the Al diffusion, leading to the autonomous formation of a spatial distribution of Al atoms. As a result, the device worked as an LED by momentum exchange between the electrons in the conduction band and the multimode coherent phonons in the DPP. The light emission principle, device fabrication, and operating characteristics of this LED were described in refs. [4, 5].

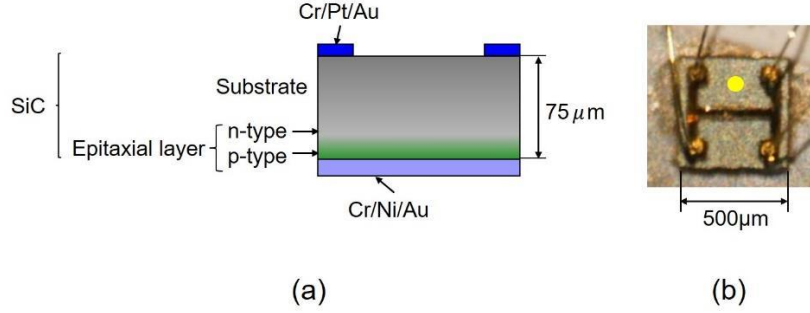


Fig. 1 Cross-sectional profile (a) and photograph (b) of a polarization rotator using a 4H-SiC crystal. The yellow circle represents the cross-sectional position of the incident light beam.

3 Performance of optical polarization rotator

To operate the device as an optical polarization rotator, a current was injected to the H-shaped electrode to inject electrons and to generate a magnetic field, simultaneously. The spatial distribution of the magnetic flux density B_{\perp} normal to the top surface (the upward green arrow in Fig. 2(a)) was estimated by numerical simulation. Figure 2(b) shows the result, where the injection current I was 30 mA. (Since the p-n homojunction was only 75 μm below the top surface, the value of B_{\perp} in this figure can be considered to be equal to that at the p-n homojunction.)

In order to measure the polarization rotation angle θ_{rot} , linearly polarized 405 nm-wavelength light was made normally incident on the top surface of this device, as schematically illustrated in Fig. 3(a). The yellow circles in Figs. 1(b) and 2(b) represent the cross-section of the incident light beam. The value of B_{\perp} at this spot was evaluated to be 1.8 mT from Fig. 2(b). That is, the relation

$$\frac{dB_{\perp}}{dI} = 0.06 \text{ (T/A)} \quad (1)$$

holds.

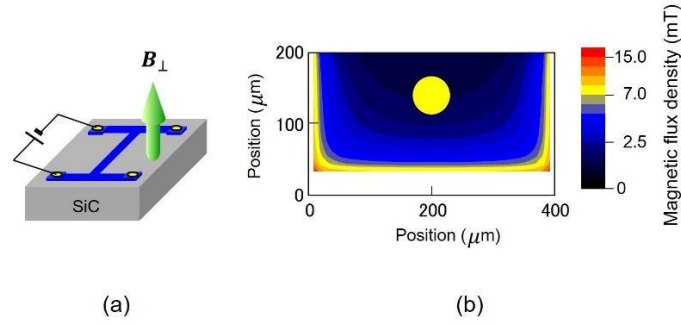


Fig. 2 Magnetic flux density generated by the current injected into the H-shaped electrode. (a) Schematic illustration of the profile of the H-shaped electrode formed of a Cr/Pt/Au stripe film on the top surface. The upward green arrow represents the normal component B_{\perp} of the generated magnetic flux density. (b) Calculated spatial distribution of B_{\perp} , where the injected current was 30 mA. The yellow circle represents the cross-sectional position of the incident light beam (Fig. 3(a)).

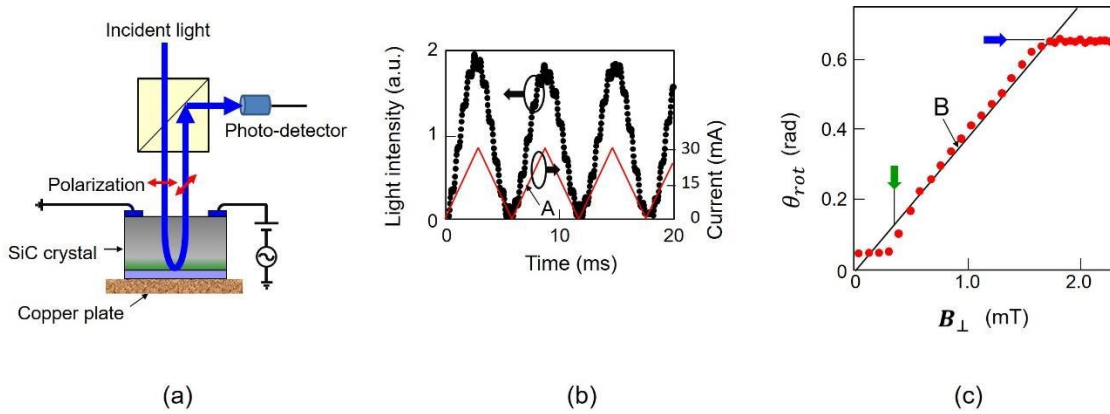


Fig. 3 Measured temporal variation of the light intensity and the estimated values of the polarization rotation angle θ_{rot} . (a) Experimental setup to measure the value of θ_{rot} . (b) Closed circles represent the measured light intensity transmitted through the Glan-Thompson prism. The red line A is the waveform of the triangular current injected into the device. Its frequency and amplitude were 166 Hz and 30 mA, respectively. (c) The relation between B_{\perp} and θ_{rot} . (The unit (π rad) written along the vertical axis of Fig. 2 in ref.[6], and also that of Fig. 8.18(b) in ref. [7], is wrong. The correct unit (rad) is written on the vertical axis of (b) above.)

The light reflected from the Cr/Ni/Au film on the rear surface propagated back to the top surface and was transmitted through a Glan-Thompson prism, after which the transmitted light intensity was measured. Closed circles in Fig. 3(b) represent the measured values of the transmitted light intensity. As shown by a red line A, the frequency and the amplitude of the triangular current injected into the H-shaped

electrode were 166 Hz and 30 mA, respectively. The measured relation between B_{\perp} and θ_{rot} was derived from this figure and is represented by the red circles in Fig. 3(c). The solid line B was fitted to these circles. From the slope of the line B, the relation

$$\frac{d\theta_{rot}}{dB_{\perp}} = 2.2 \times 10^3 (\text{deg/T}) \quad (2)$$

is derived.

From eqs. (1) and (2), the relation

$$\frac{d\theta_{rot}}{dI} = \frac{dB_{\perp}}{dI} \times \frac{d\theta_{rot}}{dB_{\perp}} \times \frac{1}{2} = 660 (\text{deg/A}) \quad (3)$$

is derived, where the value (1/2) was inserted in the left-hand side in order to evaluate the value for the one-way propagation of the light through the SiC crystal. This value corresponds to the Verdet constant, which was 10^5 - 10^6 times higher those of conventional paramagnetic materials that are transparent in the visible region [8]. This means that the present SiC crystal exhibited a gigantic magneto-optical effect.

The right-pointing blue arrow in Fig. 3(c) indicates that θ_{rot} saturated as B_{\perp} increased, as has been widely observed in conventional ferromagnetic materials. The saturated value was 0.65 rad (=37 deg). The total optical path length of the incident light propagating through the SiC crystal was 150 μm because the crystal thickness was 75 μm , as shown in Fig. 1(a). Thus, the saturated value, normalized to the unit optical path length, corresponding to the Faraday rotation angle [8], was as large as 2480 deg/cm. Furthermore, the downward green arrow indicates the threshold value of B_{\perp} , which was 0.36 mT. This value corresponds to the remanent magnetization in conventional ferromagnetic materials, and was as large as those values. The two arrows suggest that the presently used SiC crystal acquired novel properties, equivalent to those of ferromagnetic materials.

In order to find the origin of such novel ferromagnetic properties, a magnetization curve was acquired using a SQUID [6]. The results are given in Fig. 4. Here, the applied magnetic field H (Oe) was proportional to the current injected to the H-shaped electrode. The black squares represent the measured values of the magnetization M (emu/cm³) per unit volume of the SiC crystal. The solid curves were fitted to the black squares. These results clearly exhibit a hysteresis characteristic, which is inherent to ferromagnetic materials. Since these results were acquired at 27 °C, it was confirmed that the Curie temperature was estimated to be higher than 27 °C. Red open circles in this figure are the measured values before the DPP-assisted annealing was carried out, where the values of M are much smaller those of the black squares, and no hysteresis characteristic is seen.

By comparing the black squares and red open circles, it was confirmed that the semiconductor SiC crystal was made to behave as a ferromagnet as a result of the DPP-assisted annealing. This behavior originated from the formation of Al atom pairs, autonomously formed as a result of the DPP-assisted annealing. (For reference, this autonomous formation has also been confirmed in the case of B atoms in a Si-LED [2].) This origin can be understood by referring to the following two research findings:

- (1) It has been found that the triplet state of the electron orbital in an Al atom pair is more stable than the singlet state [9].
- (2) Two electrons with parallel spins in the triplet state induce the ferromagnetic characteristic [10].

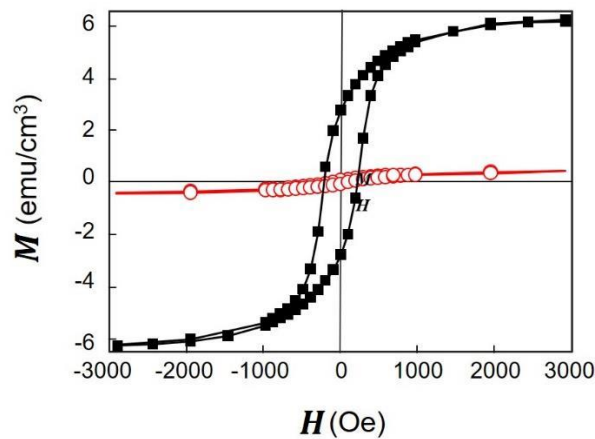


Fig. 4 Magnetization curve, measured at 27 °C. Black squares and red open circles are for the 4H-SiC crystals after and before the DPP-assisted annealing, respectively.

4 Summary

This paper investigated the gigantic magneto-optical effect in a SiC-LED fabricated by DPP-assisted annealing. This device rotated the polarization angle of linearly polarized incident light. Very large values of the Verdet constant and the Faraday rotation angle were obtained, namely, 660 deg/A and 2480 deg/cm, respectively, at a wavelength of 405 nm.

The magnetization curve, acquired at 27 °C, exhibited a clear hysteresis characteristic, by which it was confirmed that the SiC crystal behaved as a ferromagnet. This characteristic was attributed to Al atom pairs, autonomously formed as a result of the DPP-assisted annealing.

References

- [1] M. Ohtsu, *Silicon Light-Emitting Diodes and Lasers*, Springer, Heidelberg (2016) pp.16-19.
- [2] M. Ohtsu, *Silicon Light-Emitting Diodes and Lasers*, Springer, Heidelberg (2016) pp.15-102.
- [3] M. Ohtsu, *Silicon Light-Emitting Diodes and Lasers*, Springer, Heidelberg (2016) pp.126-131.
- [4] T. Kawazoe and M. Ohtsu, *Appl. Phys. A*, **115** (2014) pp.127-133.
- [5] M. Ohtsu, *Silicon Light-Emitting Diodes and Lasers*, Springer, Heidelberg (2016) pp.83-101.
- [6] T. Kawazoe, N. Tate, and M. Ohtsu, "SiC magneto-optical current-transformer applicable to a polarization rotator using dressed photons," Abstract of the 22nd International Display Workshops, Dec. 9-11, 2015, Otsu, Japan, PRJ3-5L.
- [7] M. Ohtsu, *Silicon Light-Emitting Diodes and Lasers*, Springer, Heidelberg (2016) pp.132-138.
- [8] *Chronological Scientific Tables*, the 77th edition, (ed)National Astronomical Observatory of Japan, Maruzen Co., Tokyo, Japan (2004) p.449
- [9] T.H. Upton, "Low-lying valence electronic states of the aluminum dimer," *J. Phys. Chem.*, **90** (1986) pp.754-759.
- [10] A. Rajca, "Organic Diradicals and Polyradicals: From Spin Coupling to Magnetism?," *Chem. Rev.*, **94** (1994) pp.871-893.